Virtual Treaded Tire Simulation as a Design Predictive Tool: Application to Tire Hydroplaning

M. Donatellis, E. Gelosa, and R. Sangalli

Pirelli Tyres

M. Spinelli and R. Vitali

ABAQUS Italia

Abstract: In the last decades FEA simulation has been used intensively within the tire development process with the aim to predict and improve tire performance. Thanks to the speed-up in computing times recently obtained on the HW side, the introduction of tread pattern in tire modeling has been made possible and affordable, allowing the tire FEA analyst to perform treaded tire virtual prototyping and give design guidelines in "industrial" times.
Abaqus has been developing and implementing new features able to represent a treaded tire in rolling conditions and in release 6.7-EF announced a Coupled Eulerian-Lagrangian (CEL) explicit approach to simulate fluid-structure interaction.
Pirelli developed a new simulation procedure for treaded tire analysis, based on Abaqus new features ****STEADY STATE TRANSPORT, PERIODIC*** *and CEL techniques, and fitted it in the standard design process, starting from tire CAD drawing up to the application of tire dynamic service conditions. This modeling procedure has been applied to investigate FEA potentiality in predicting an important tire performance index strongly related to tread pattern geometry, that is tire hydroplaning.*
Hydroplaning is a dynamic phenomenon the tire undergoes while rolling on a wet road, when water penetrates under footprint, causing a progressive reduction of the contact patch at increasing rolling speed, thus affecting car/passengers safety.
Using Abaqus ****SST, PERIODIC*** *Pirelli built up a "virtual" test bench which makes the treaded tire roll in steady state free rolling conditions; the model, rolling at specified forward speed, is then imported into Abaqus/Explicit and coupled with a fluid domain using the CEL approach. Contact patch, footprint pressures and resulting hub forces, which depend on tread pattern capability to drain water, can be numerically monitored and evaluated as a function of speed until critical conditions are identified and considered as a warning index for tire potential hydroplaning.*
In this paper Abaqus application is shown to different tread pattern geometries with the aim to assess FEA model robustness; more specifically, effects of speed and pattern geometry have been investigated. Simple laminar fluid cases (from literature) have been also simulated for sake of basic assessment of the CEL methodology.
Computed results are shown and compared with experimental tests performed at Pirelli facilities.

Keywords: Hydroplaning, Tires, Coupled Analysis, Hyperelasticity, Rubber.

1. Introduction

Tire hydroplaning analyses are challenging simulations because of all the complexities of the components involved in this high non-linear dynamic event (different type of materials: rubber, metal, nylon, geometric nonlinearities, contact interactions in between: the tire and the road, the treads themselves, the water and the tire and the road) affect the phenomenon.

A software program able to treat simultaneously the fluid and structural behaviors and the interactions in between them should be the best tool for this class of applications (Okano, 2001). Up to now, many applications have been done through sequentially coupling of CFD and FEM programs, (Grogger, 1996), (Grogger, 1997), (Janajreh, 2007), (Lee, 1998), (Seta, 2000). This technique requires a lot of computational efforts because of the need: (a) to couple the programs (many times using a third coupling software), (b) to exchange the data in between them very frequently due to the continuous variations of the interacting domains, and (c) the domains' interacting surfaces must be defined a priori (Dinescu, 2006). Other difficulties are represented by the nature of the shape of the tread patterns (very complex and small, compared to the overall dimension of the structure) that requires a lot of efforts to produce the mesh (generally very fine) and the initial conditions of the rolling tire before to impact the water that are computed with a transient explicit analysis, very time consuming from performance point of view.

Nowadays, the Abaqus' solution made by the steady-state transport analysis in Abaqus/Standard, the model/results transfer from Abaqus/Standard to Abaqus/Explicit and the new Coupled Eulerian-Lagrangian (CEL) technique included in Abaqus/Explict with its general contact algorithm allows to overcome all the above mentioned difficulties offering to the designers a unique software environment where the tire virtual prototyping can be successfully performed with the benefits of reducing R&D costs and shortening time-to-market.

In the present paper, after an introduction to the CEL approach and the validation of its Eulerian functionality, the analysis carried on different treaded tires is presented.

2. The Coupled Eulerian-Lagrangian (CEL) approach in Abaqus

Abaqus/Explicit offers the Coupled Eulerian-Lagrangian (CEL) approach where the Eulerian implementation (only available for three-dimensional problems) is based on the volume-of-fluid method. In this method, material is tracked as it flows through the mesh by computing its Eulerian volume fraction (EVF) within each element (Abaqus, 2008). By definition, if a material completely fills an element, its volume fraction is one; if no material is present in an element, its volume fraction is zero. Eulerian elements may simultaneously contain more than one material. If the sum of all material volume fractions in an element is less than one, the remainder of the element is automatically filled with "void" material. Void material has neither mass nor strength.

Volume fraction data are computed for each Eulerian material in an element. Within each time increment, the boundaries of each Eulerian material are reconstructed using these data. The interface reconstruction algorithm approximates the material boundaries within an element as simple planar facets. This assumption produces a simple, approximate material surface that may be discontinuous between neighboring elements. Therefore, accurate determination of a material's location within an element is possible only for simple geometries, and fine grid resolution is required in most Eulerian analyses.

The Eulerian time incrementation algorithm is based on an operator split of the governing equations, resulting in a traditional Lagrangian phase followed by an Eulerian, or transport, phase. This formulation is known as “Lagrange-plus-remap” (Figure 1). During the Lagrangian phase of the time increment nodes are assumed to be temporarily fixed within the material, and elements deform with the material. During the Eulerian phase of the time increment deformation is suspended, elements with significant deformation are automatically remeshed, and the corresponding material flow between neighboring elements is computed. At the end of the Lagrangian phase of each time increment, a tolerance is used to determine which elements are significantly deformed. This test improves performance by allowing those elements with little or no deformation to remain inactive during the Eulerian phase.

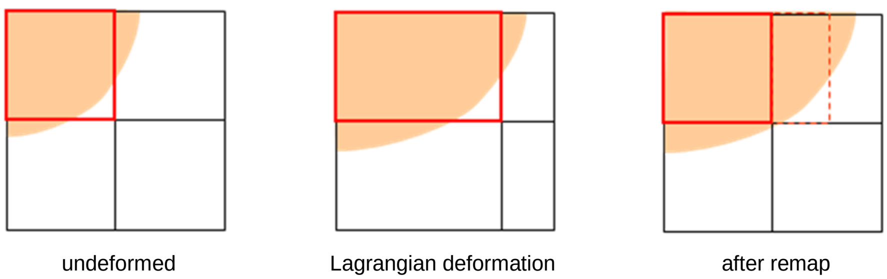

Figure 1. The Eulerian time incrementation algorithm.

Interactions in between Eulerian material instances (Eulerian-to-Eulerian) as well as Eulerian and Lagrangian instances (Eulerian-Lagrangian) can be considered.

The Eulerian-to-Eulerian is computed automatically (no need to define a contact interaction) with a sticky behavior because of the kinematic assumption that a single strain field is applied to all materials within an element. Tensile stress can be transmitted across an interface between two Eulerian materials, and no slip occurs at these interfaces.

More complex contact interactions (Eulerian-Lagrangian) can be simulated when one of the contacting bodies is modeled using Lagrangian elements. This powerful capability supports applications such as fluid-structure interaction, where an Eulerian fluid contacts a Lagrangian structure. The implementation of Eulerian-Lagrangian contact is an extension of general contact in Abaqus/Explicit. The general contact property models and defaults apply to Eulerian-Lagrangian contact. For example, by default, tensile stresses are not transmitted across an Eulerian-Lagrangian contact interface, and the interface friction coefficient is zero. Specifying automatic contact for an entire Eulerian-Lagrangian model allows for interactions between all Lagrangian structures and all Eulerian materials in the model. Eulerian surfaces can be defined to create material-specific interactions or to exclude contact between particular Lagrangian surfaces and Eulerian materials. The Eulerian-Lagrangian contact formulation is based on an enhanced immersed boundary method. In this method the Lagrangian structure occupies void regions inside the Eulerian mesh. The contact algorithm automatically computes and tracks the interface between the Lagrangian structure and the Eulerian materials. A great benefit of this method is that there is no need to generate a conforming mesh for the Eulerian domain. In fact, a simple regular grid of Eulerian elements often yields the best accuracy.

Eulerian-Lagrangian contact also supports failure and erosion in the Lagrangian body. Lagrangian element failure can open holes in a surface through which Eulerian material may flow. Erosion of Lagrangian solid elements exposes new element faces, which are automatically included in the Lagrangian surface definition.

Eulerian-Lagrangian contact constraints are enforced using a penalty method, where the default penalty stiffness parameter is automatically maximized subject to stability limits.

3. Validation of the CEL approach

The Eulerian capability of Coupled Eulerian-Lagrangian (CEL) technique in Abaqus/Explict is not intended to compete with CFD solvers; mainly because, within the CFD applications, laminar effects can be modeled while turbulence effects cannot, and secondly because the class of problems that can be treated with CEL is wider than the CFD applications (e.g. Multi-pass rolling of an I-bar). Therefore, a direct comparison should be avoided. Nevertheless, this paragraph shows the results that can be obtained with the Eulerian capability of CEL technique applied on the following two laminar benchmark problems:

- Fully-developed laminar flow in a rectangular channel
- Laminar fluid flow across a circular cylinder

3.1 Fully-developed laminar flow in a rectangular channel

The objective of this example is to study the velocity's distribution in a rectangular channel subjected a laminar flow (Figure 2).

H=0.1 [m] Viscosity=1.0 [Kg/ms]

L=1.0 [m] Density=1000.0 [Kg/m^3]

V_o=0.04 [m/s] $Re_h = \dfrac{\rho V L}{\mu} = 4$

Figure 2. Laminar flow in a rectangular channel.

The results obtained shown in Figure 3 highlight the good agreement with the analytical solution as well as put in evidence the need to use a fine mesh to capture the boundary layer.

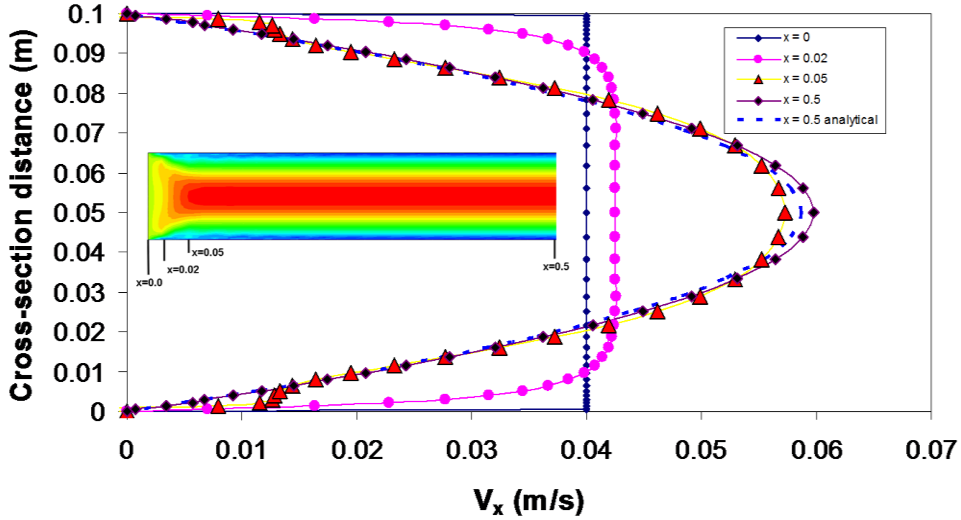

Figure 3. Velocity profile in channel flow.

3.2 Flow across a circular cylinder

The purpose of this test is to analyze the velocity profile and the coefficient of pressure around a circular cylinder in a two-dimensional flow of an incompressible fluid. (Grove, 1964)

D=1.0 [m] Viscosity=1.0 [Kg/ms]

V_o=1.0 [m/s] Density=40.0 [Kg/m^3]

$$Re_h = \frac{\rho V L}{\mu} = 40$$

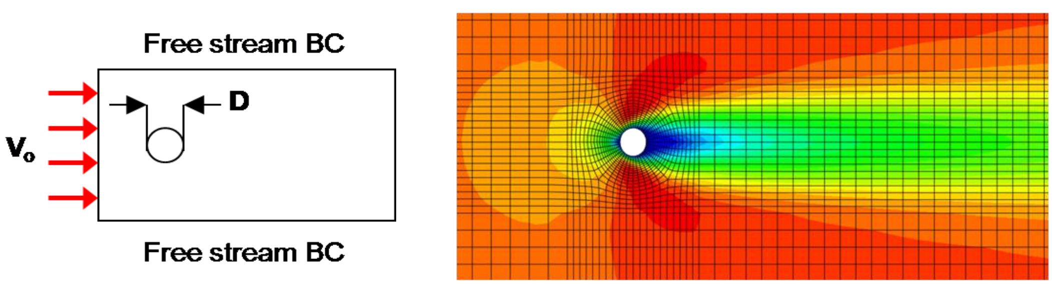

Figure 4. Flow across a circular cylinder: velocity profile.

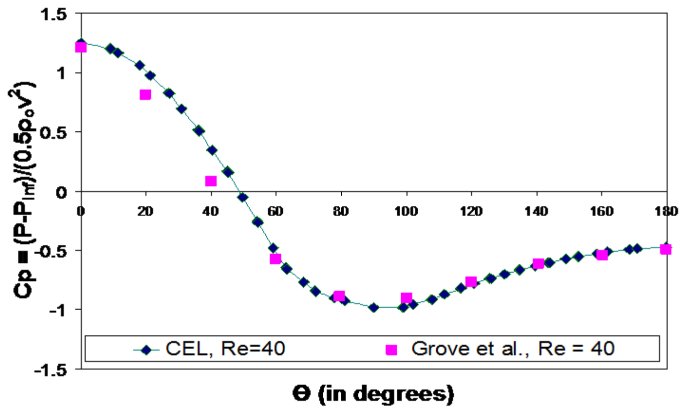

Figure 5. Variation of coefficient of pressure (Cp) with angle Θ* in degrees.

4. Pirelli treaded tire modeling procedure

4.1 Modeling set-up

Main requirement for an industrial development tool is to be based on robust procedure that can be routinely applied within the framework of well defined production process.

Virtual prototyping: computational time costs reduction requires the analysts to simulate only the key features describing the phenomenon under investigation. Material stiffness non linearity has to be taken into account both for rubber and reinforcements. Polynomial strain energy constitutive law is commonly used for rubber and we choose **`*HYPERELASTIC, N=1`** for all compounds.

Textile and steel ply has been described using **`*REBAR LAYER`** option in conjunction with Marlow model (**`*HYPERELASTIC, MARLOW`**) for fibers material description. No temperature stiffness dependency has been considered for any material.

Geometry approximation requires a much more detailed description. We can basically split tire in axi-symmetric structural part and a non symmetrical part: the tread.

Tread geometry is obtained assembling a sequence of pitches (Figure 6a) each one spanning different angle. The proper sequence of tread pitches is optimized to reduce, mainly, noise and wear.

Just for sake of time costs reduction, we made here the assumption the tread has a periodic symmetry. Defining the average pitch dimension we can describe a treaded tire repeating n time the single tire slice (Figure 6b).

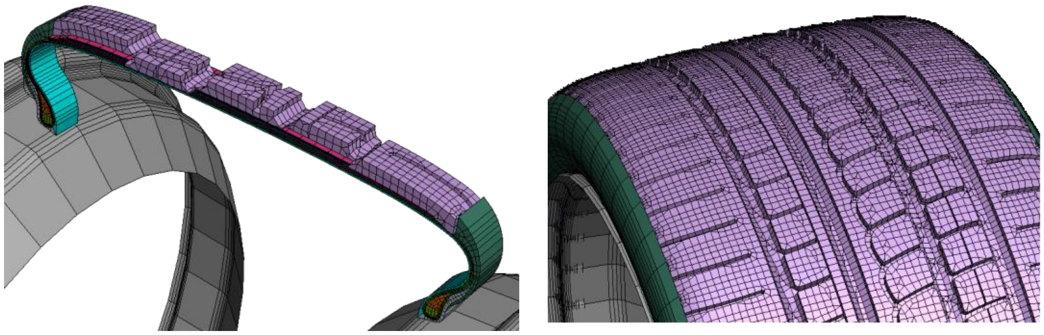

(a) (b)

Figure 6. Tire model assembling: (a) single tread pitch, (b) full treaded tire.

Abaqus ***SST, PERIODIC** has been designed at this purpose to simulate rotating periodic structure using a traditional Lagrangian.formulation. The steady-state transport analysis capability in Abaqus/Standard uses a reference frame that is attached to the axle of the rotating cylinder. An observer in this frame sees the cylinder as points that are not moving, although the material of which the cylinder is made is moving through those points. This description can be viewed as a mixed Lagrangian/Eulerian method, where rigid body rotation is described in a spatial or Eulerian manner, and deformation, which is now measured relative to the rotating rigid body, is described in a material or Lagrangian manner. It is this kinematic description that converts the steady-state moving contact problem into a purely spatially dependent simulation.

Assuming tread periodicity, not only one has the chance to use ***SST, PERIODIC** capabilities but also one is required to mesh only one tread pitch (instead of the complete geometry).

Tread Mesh Generation: it's well known that rubber materials are nearly incompressible and require special attention on finite element formulation. Usually we rely on H element (8-node linear brick, hybrid constant pressure), but due to Abaqus/Explicit limitation we must stick on reduced integration elements. To obtain a smooth pressure distribution for footprint area, as for H-element, a very fine mesh is mandatory.

As far as concern mesh technique, hexa elements should be preferred in contact region, in particular for tread. Moreover ***SST, PERIODIC** technique requires also the mesh to be periodic. Abaqus/CAE doesn't allow achieving mesh periodicity for any arbitrary complex geometry in an industrial time frame using an automated procedure; that'why another commercial 3D mesh-generator has been preferred.

It is anyway very time consuming a full-hexa-periodic tread mesh generation. Best results have been obtained using hexa-dominant periodic mesh that means allow the algorithm to insert tetra, prism or degenerated hexa to fill sharp corner geometry.

Figure 7 shows an overall description of pre-processing phase.

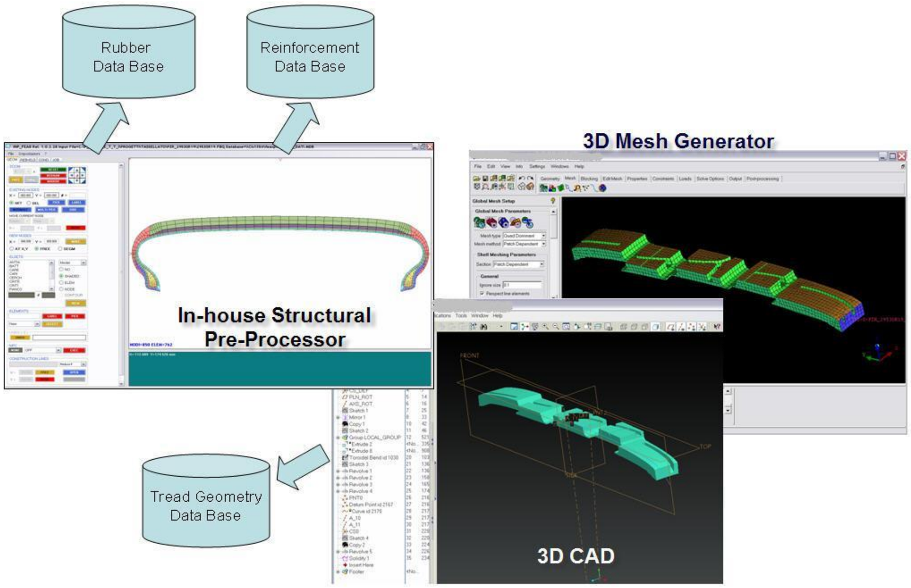

Figure 7. Pre-processing phase.

Finally, while the structural mesh sizing has been driven by the common tire analyst's experience, the fluid domain dimension and its mesh discretization has been chosen to optimize results consistency and computer timings.

4.2 Analysis procedure

Fluid-structure interaction (hydroplaning simulation) is the last step of calculation sequence.

Treaded tire model will be subjected to service condition using Abaqus/Standard: once the geometry has been generated taking advantage of periodicity, the tire will be mounted on the proper rim and inflated at a given pressure. A vertical load is then applied and, using `*SST, PERIODIC` procedure, the tire will reach a stationary rolling condition at constant travelling speed.

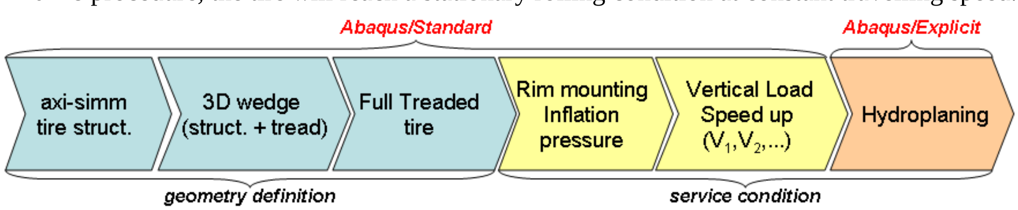

Figure 8. Calculation sequence.

Rolling tire is finally imported into Abaqus/Explicit to run the non-stationary fluid structure interaction impact. See calculation sequence in Figure 8. Within Abaqus/Explicit environment not only the fluid domain is added but also a dashpot element is defined, connecting rim to car structure to simulate the damping suspension characteristic (Figure 9).

The calculation procedure doesn't predict automatically the "hydroplaning speed". Such values will results analysing footprint shape and road reaction forces. To this purpose the calculation procedure implies to repeat the **`*SST, PERIODIC`** and /Explicit simulations a reasonable number of speeds in a range around the expected hydroplaning critical velocity.

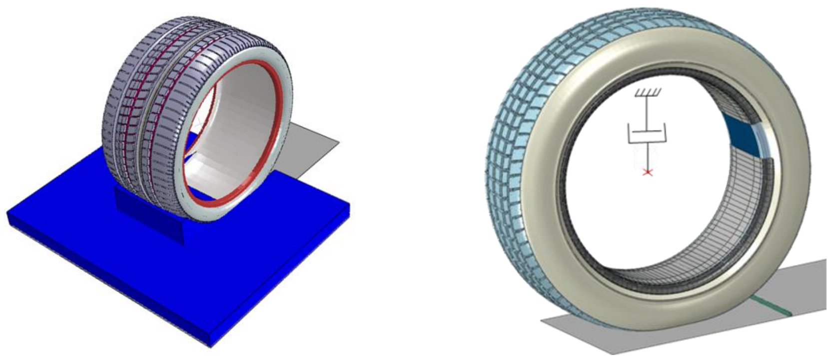

(a) **(b)**

Figure 9. Example of Abaqus model: (a) treaded tire structure and fluid domain, (b) tire model and suspension set-up.

For a specified forward speed a single Abaqus/Explicit run is performed, representing the water-tire transient impact simulation. Depending on the tread pattern capability to drain fluids, part of the water volume can flow into the grooves; at the same time, due to the dynamic water pressure against the tire deformable structure, a lift force arises and increases; therefore water can also progressively penetrate under the tire footprint patch (Figure 10), thus reducing the original contact area between tire and road, until a stable lift force is reached and considered as a steady state value for the rolling prescribed conditions. Figure 11 shows time history of vertical reaction force at road, which highlights the steady state lift force.

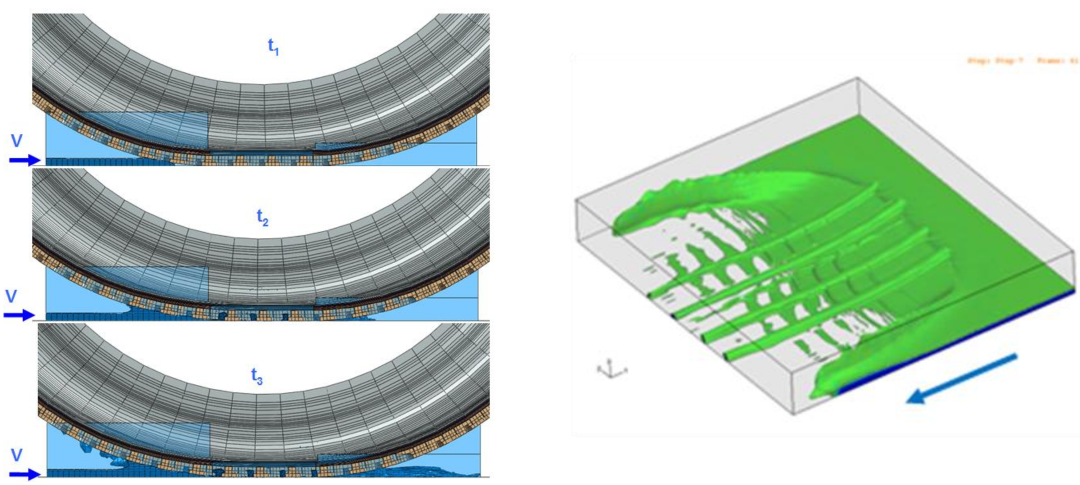

Figure 10. Water flow towards (left) and around (right) the treaded tire structure.

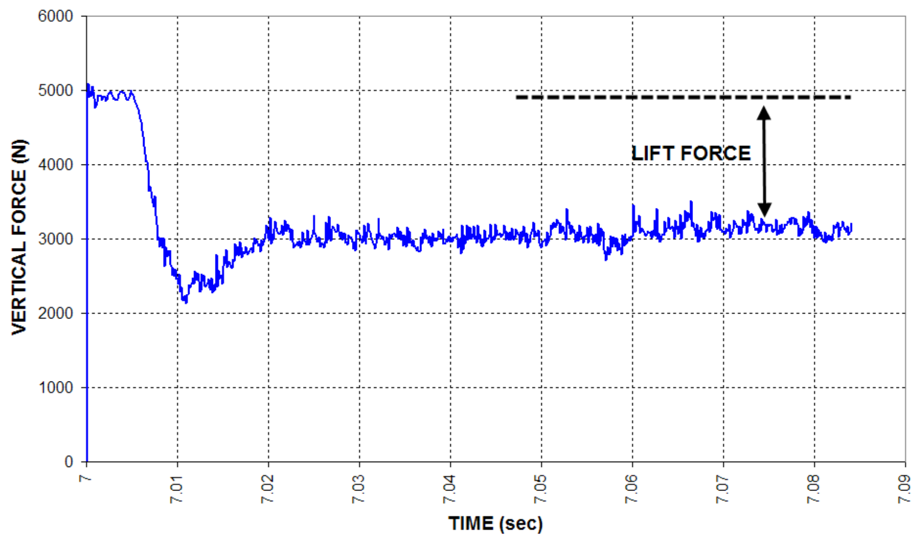

Figure 11. Time history of vertical reaction force at road.

Corresponding footprint patch is an estimation of the steady state tread-contact area associated with the defined speed conditions; Figure 12 shows change of footprint patch from full tread-road contact (initial rolling, before water impact) to final, partial, tread-road contact (rolling through water).

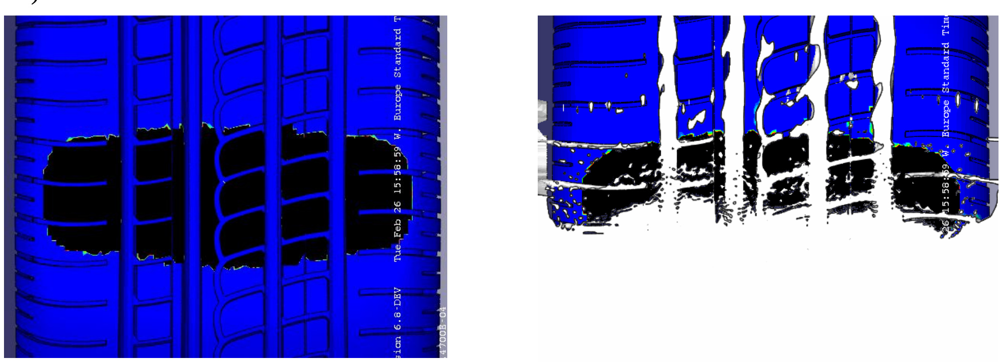

Figure 12. Footprint patches: initial (left) full contact, and final (right) partial contact.

5. Application to tread pattern geometries

5.1 Analysis results

The developed simulation methodology has been applied to evaluate 2 different tread pattern geometries (pattern A and B) on the same tire body structure. Figure 13 highlights the corresponding static footprint patches and pressures.

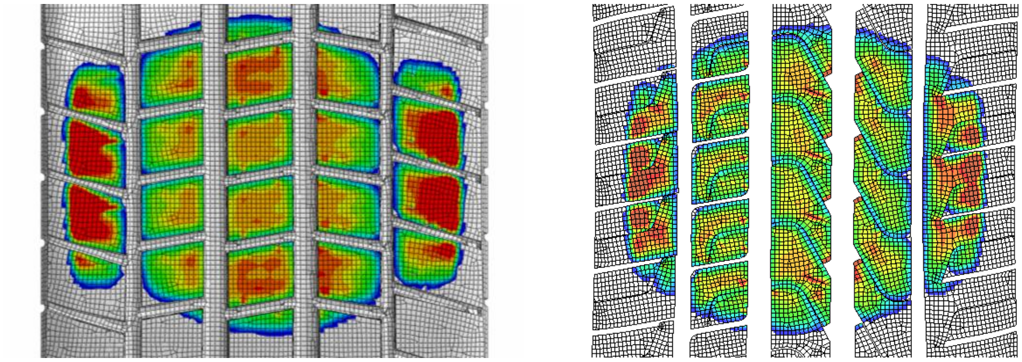

Figure 13. FEA static footprint patches and pressures for tread pattern A and B.

Multiple dynamic simulations at several forward speeds have been run for both tire models and corresponding evolution/drop of vertical reaction force at road was monitored until steady conditions; see Figure 14.

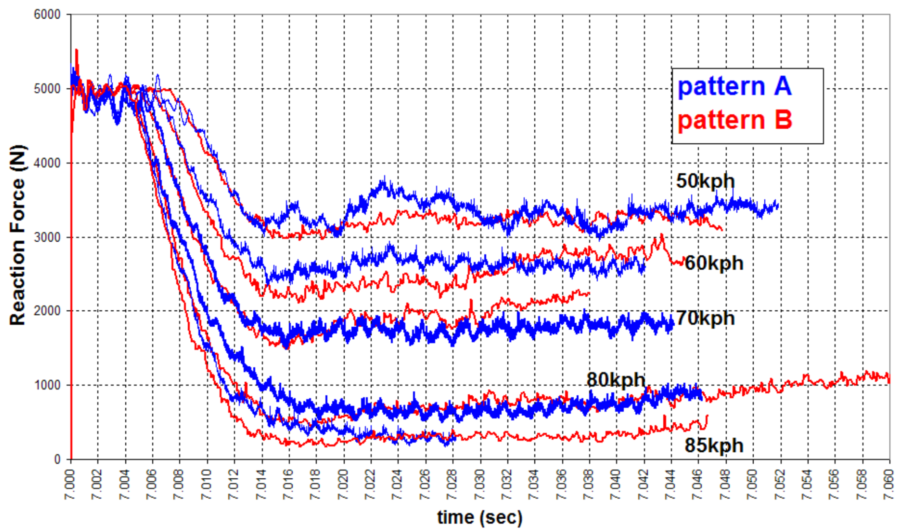

Figure 14. FEA static vertical force at road vs. time at different forward speed.

Figure 15 shows corresponding change of tire-road contact patch from static conditions to dynamic rolling ones at different forward speeds. Contact pressure contour maps clearly show that water penetrates under the leading edge causing a reduction in the footprint length and a progressive loss of contact with road. At V=85kph the whole contact area is almost disappeared for both pattern A and B, thus detecting that they are approaching a critical speed Vcr which is correlated with hydroplaning phenomenon occurrence (for straight-ahead traveling).

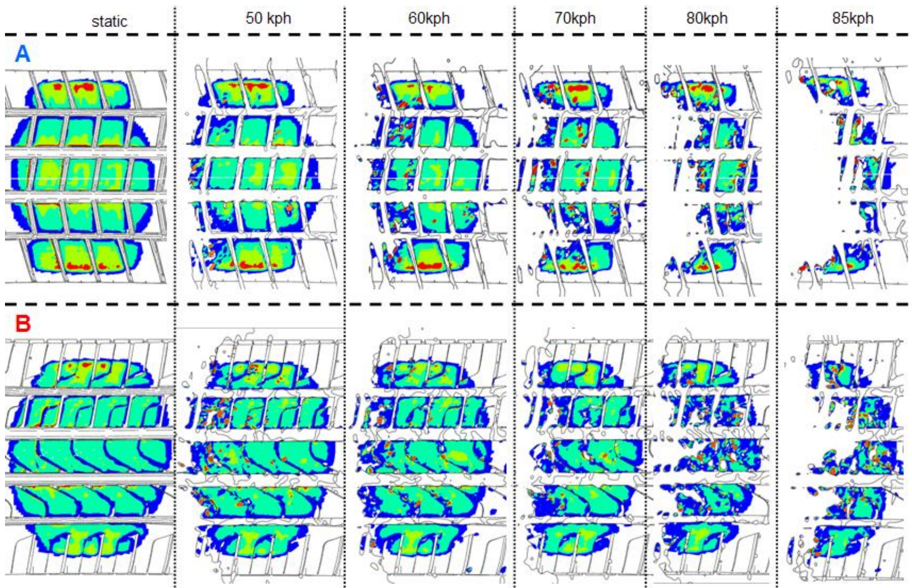

Figure 15. FEA footprint pressures (pattern A and B) at increasing speeds.

The calculated trend of tread/road contact reduction is considered as a tire behavior index by tire analyst and reasonably used to evaluate tire hydroplaning performance (straight ahead).

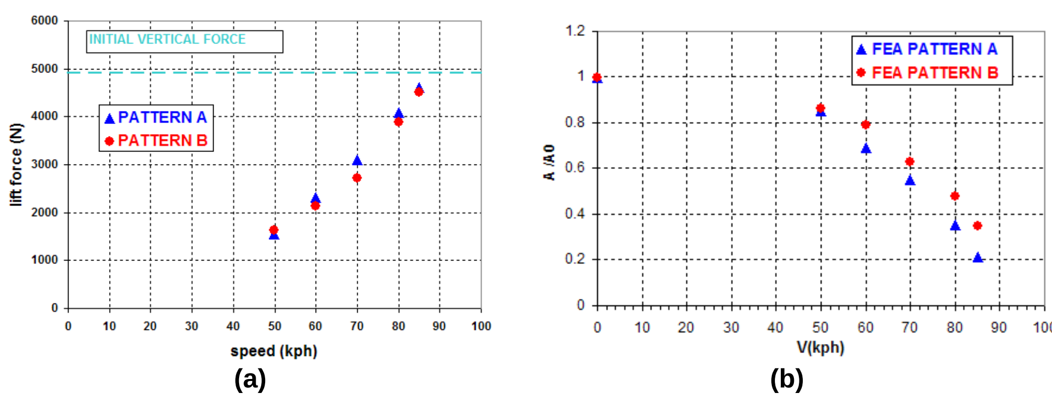

Figure 16. (a) Calculated lift force vs. speed, and (b) calculated A/A0 vs. speed.

Additional FEA results and indexes can be extracted with the aim of numerical comparison and ranking. Figure 16a shows calculated lift force as a function of speed, obtained as described in Figure 11; moreover the change in the tread contact surface can be expressed in terms of ratio A/A0 where A is the contact area at the current speed, A0 is the footprint area in static conditions (V=0), see Figure 16b.

The two graphs confirm that the 2 tire models seem to approach to the same critical speed but with a different behavior at intermediate speeds: pattern A shows to loose more contact than pattern B even when V< Vcr.

5.2 Comparison with experimental tests

To evaluate consistency of the described Abaqus modeling approach, real tires have been carved with same tread patterns as simulation and tested on vehicle. A specific glass-pit test at Pirelli test track allows obtaining contact patch camera pictures when tire is rolling at constant speed on a prescribed water thickness (7 mm) which is placed on a transparent plate. Pictures in Figure 17 clearly show qualitatively how water push under tread blocks in the leading edge and contact changes for pattern A and B.

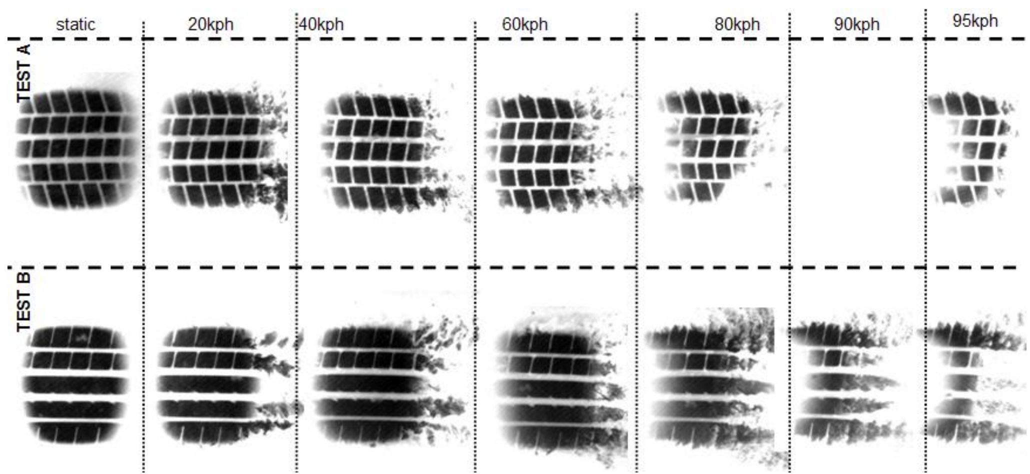

Figure 17. Camera pictures from glass pit test.

Camera pictures have also been processed so to identify tread contact area, for sake of quantitative comparison with FEA results. Figure 18 shows experimental pictures and simulated ones, converted into black.

Despite some discrepancies even in static conditions, also due to the vehicle suspension (camber) setting which has not been considered yet in the simulations, FEA results demonstrate they properly catch the progressive reduction of tread/contact area when increasing tire/vehicle speed. The 2 tires show a quite similar experimental behavior as to tread contact loss.

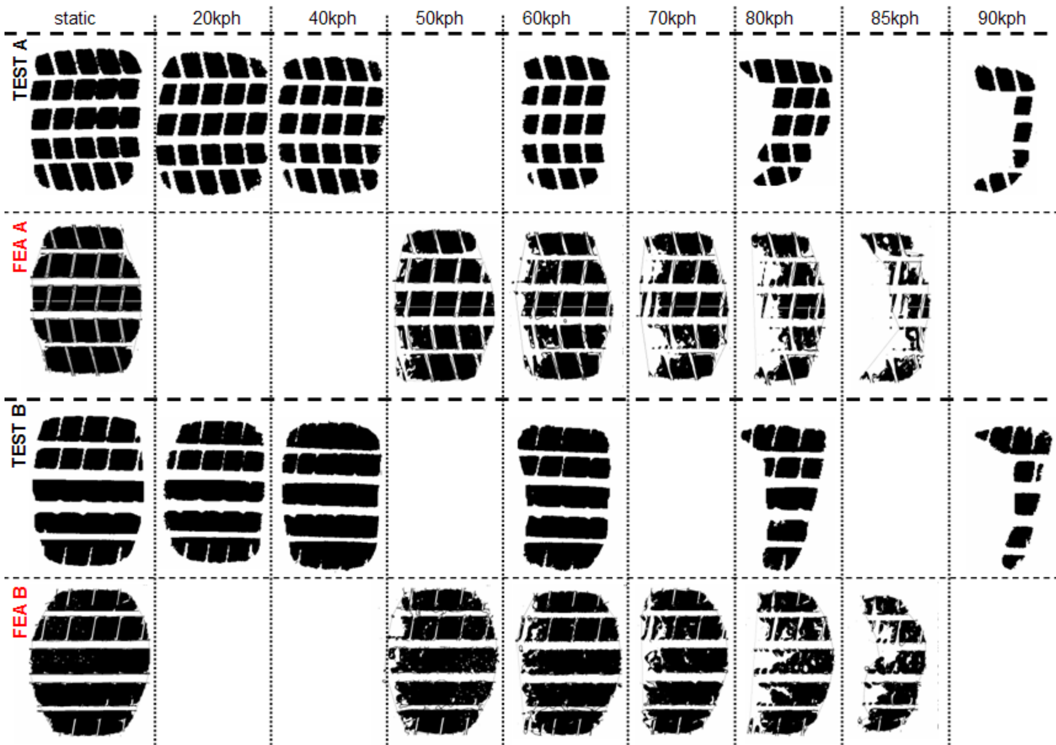

Figure 18. Comparison between camera pictures (TEST) and calculated footprint (FEA) for tread A and B.

To better assess tire hydroplaning behavior, a hydroplaning test has also been done on vehicle equipped with same tires A and B as simulated. Vehicle proceeds straight on a track pool continuously filled with water to ensure a constant water depth (7 mm); driving acceleration is applied by the driver until a critical speed is reached and recorded when the tire completely looses contact with road. Critical speed measured in this test for Tire A and B showed approximately the same value (ΔV_{crit} lower than test accuracy), therefore hydroplaning test on vehicle once again shows that pattern A and B are quite similar as already detected by glass-pit test (Figures 17 and 18).

As a conclusion both experimental tests on tires confirm simulation results, that is pattern A and B have a very similar hydroplaning critical speed, with a sort of different “loss of contact history” at lower speed (Figures 16b and 18).

6. Conclusions

A new predictive tire finite element model based on Abaqus CEL capability has been presented and applied on two different tread patterns to investigate hydroplaning phenomenon on straight-ahead traveling.

The new tool provides numerical results in good agreement with hydroplaning experimental data.

Great effort has been made to fit the new simulation procedure into the standard design process with the aim to shorten as much as possible the virtual prototyping timings (model generation and analysis execution).

The new predictive tool allows the tire analyst to ensure that designed treads patterns fulfill hydroplaning specific target requirements. This assessment can be accomplished in the very early phase of a new tire development; in conjunction with other FEA tools able to predict different performances indexes (cornering stiffness, rolling resistance, dynamic footprint, etc.), it allows optimization of tread pattern geometry, gives guidelines on the best design choices, thus avoiding the need to build up many physical tire prototypes with a consequent positive impact on R&D cost reduction.

7. References

1. Abaqus V6.8-EF, Dassault Systems SIMULIA Corp. Providence, RI, USA (2008)
2. C. Dinescu, C. Hirsch, B. Leonard, Ö. U. Baran, A.W. Platschorre, R. Alessio, D. Belluzzo, “Fluid-Structure Interaction Model for Hydroplaning Simulations”, SAE paper 2006-01-1190
3. H. Grogger and M. Weiss, “Calculation of the Three-Dimensional Free Surface Flow Around an Automobile Tire”, Tire Sci. and Technol. 24 39 (1996)
4. H. Grogger and M. Weiss, “Calculation of the Hydroplaning of a Deformable Smooth-Shaped and Longitudinally-Grooved Tire”, Tire Sci. and Technol. 25 265 (1997)
5. Grove et al., “An Experimental Investigation of the Steady Separated Flow Past a Circular Cylinder”, Journal of Fluid Mechanics, Vol 19, 1964, pp. 60-80
6. I. Janajreh and C. Ghenai, “Numerical modeling of fluid impigment of a rolling tire”, 172nd Technical Meeting of the Rubber Division of the American Chemical Society, Inc. Cleveland, OH (2007)
7. K. S. Lee, “Effects of Sipes on the Viscous Hydroplaning of Pneumatic Tires”, Tire Sci. and Technol. 26 23 (1998)
8. T. Okano and M. Koishi, “A New Computational Procedure to Predict Transient Hydroplaning Performance of a Tire”, Tire Sci. and Technol. 29 2 (2001)
9. E. Seta, Y. Nakajima, T. Kamegawa, and H. Ogawa, “Hydroplaning Analysis by FEM and FVM: Effect of Tire Rolling and Tire Pattern on Hydroplaning” , Tire Sci. and Technol. 28 140 (2000)

8. Acknowledgment

The authors like to thank Brad Maker, Harish Surendranath, and Sharat Prasad of SIMULIA HQ for their help, support, and valuable collaboration.